



Frontiers in Photonics Spot Light

Bahman Anvari¹, Costantino De Angelis², Shujuan Huang³, Natasha Litchinitser⁴, Ting-Chung Poon⁵, Giacomo Scalari⁶, Bryce S. Richards^{7,8} and Marco Peccianti^{9*}

¹Department of Bioengineering, University of California, Riverside, Riverside, CA, United States, ²Department of Information Engineering, University of Brescia, Brescia, Italy, ³Sustainable Energy Research Centre, School of Engineering, Macquarie University, Sydney, NSW, Australia, ⁴Department of Electrical and Computer Engineering, Duke University, Durham, CA, United States, ⁵Bradley Department of Electrical and Computer Engineering, Virginia Tech, Blacksburg, VA, United States, ⁶Institute of Quantum Electronics, ETH Zürich, Switzerland, ⁷Institute of Microstructure Technology, Karlsruhe Institute of Technology (KIT), Karlsruhe, Germany, ⁸Light Technology Institute, Karlsruhe Institute of Technology, Karlsruhe, Germany, ⁹Emergent Photonics (EPic) Laboratory, Department of Physics and Astronomy, University of Sussex, Brighton, United Kingdom

Recognizing remarkable achievements and innovations is an important mission in scientific dissemination. The editors of Frontiers in Photonics would like to acknowledge and give visibility to some of the best recent research outputs and to their authors in this spot-light review.

Keywords: photonics highlights, biophotonics, nonlinear optics, photovoltaic materials, optical nanostructures, holography, terahertz, luminescent materials

OPEN ACCESS

Edited by:

Nikolaos K. Efremidis,
University of Crete, Greece

Reviewed by:

Fan O. Wu,
University of Central Florida,
United States
Yannis Kominis,
National Technical University of
Athens, Greece

*Correspondence:

Marco Peccianti
m.peccianti@sussex.ac.uk

Specialty section:

This article was submitted to
Nonlinear Optics,
a section of the journal
Frontiers in Photonics

Received: 12 January 2022

Accepted: 25 January 2022

Published: 09 March 2022

Citation:

Anvari B, De Angelis C, Huang S,
Litchinitser N, Poon T-C, Scalari G,
Richards BS and Peccianti M (2022)
Frontiers in Photonics Spot Light.
Front. Photonics 3:853456.
doi: 10.3389/fphot.2022.853456

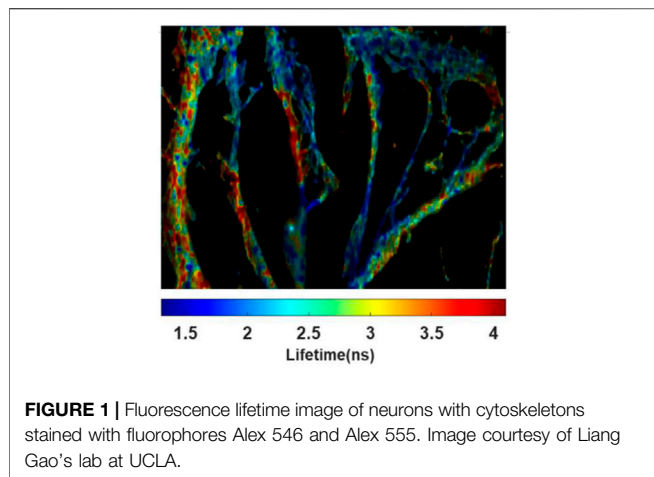
INTRODUCTION

A primary mission for Frontiers in Photonics is to recognize that the progress of the field is the main research output. Such progress is marked by results progressively answering key scientific questions within much larger challenges. The ways such outcomes are created are not a homogenous set of methods and approaches. They are often the result of a long-standing research plan, but they can also result from research endeavors serendipitously steering from their original aim. While considering a research output important for its pivotal place in a much bigger scheme appears a simple and reasonable line of thought, it involves a number of challenging aspects. The pathway to the impact of many works can be long and, sometimes, unexpected. This makes providing a snapshot in a specific moment of time of works that capture the attention for specific disruptive elements a difficult practice.

Yet, showcasing particularly impressive research outputs and their authors is a compelling objective, not only because rightfully recognizing outstanding efforts can fuel the passion for specific research but also because reaching out from the specific community is always a central challenge, especially for early-career researchers.

With this paper, we want to briefly spot-light a few selected works that, in our view, carry disruptive and transformative elements within the vastity and diversity of the photonics domain.

While in biophotonics, Feng et al. defines new speed-benchmarks for bioimaging, Koshelev et al. engage in a fundamental step forwards in the efficiency of nonlinear optics via nano-resonator-mediated enhancements. Similarly intriguing, Jiang et al. demonstrate a generational improvement in Tin-based perovskites for solar energy harvesting, essential in reducing the reliance on lead-based perovskites technologies with a lower-toxicity alternative, whereas Li and coworkers demonstrated that the property of exotic Dyakonov surface waves can be exploited for optical manipulation. In optical information processing and holography, Bang et al. demonstrate a virtual reality near-eye display that can fit a sunglasses-like form factor, while Tahara and coworkers feature a palm-sized Fresnel incoherent correlation holography system. Concluding, Khalatpour et al. take a major step towards the integration of exceptionally bright terahertz



sources in portable devices whereas Roh et al. investigate the inherent limit of photonic down-conversion in solar energy harvesting.

SPOT LIGHT IN BIOPHOTONICS

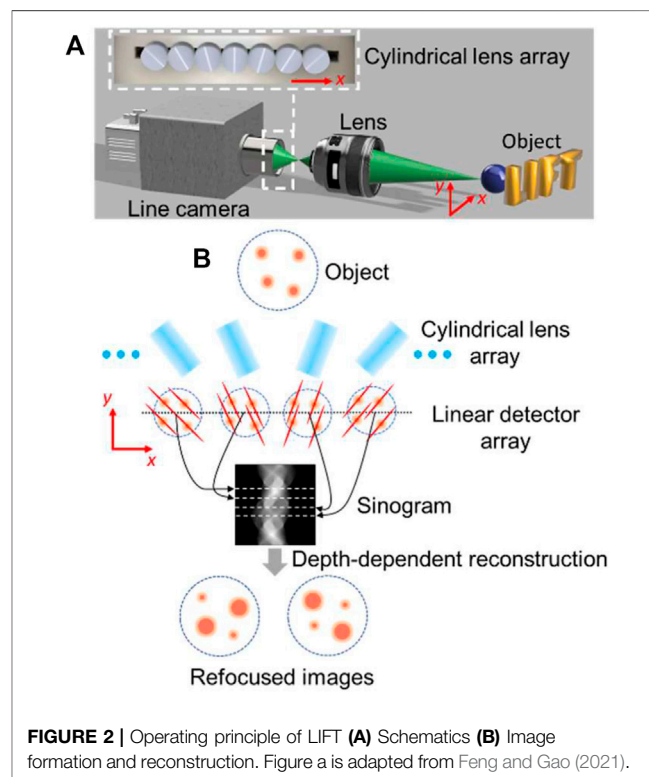
Ultrafast light field tomography for snapshot transient and non-line-of-sight imaging, by X. Feng and L. Gao (Feng and Gao, 2021).

Space and time, two key physical dimensions, constitute the basis of modern metrology. In bioimaging, as recognized by the 2014 Nobel Prize in chemistry, there have been breathtaking advances in improving spatial resolution, resulting in an impressive arsenal of nanoscopy tools that can break the diffraction limit of light. Despite the importance, the pursuit of a high temporal resolution in bioimaging has only recently been gaining attention. The motivation to develop methods for ultrafast imaging originates from the landscape shift of contemporary biology from morphological explorations and phenotypic probing of organisms to seeking quantitative insights into underlying mechanisms at molecular levels. The transient molecular events occur at a timescale varying from a few nanoseconds that molecules glow in their “fluorescence lifetime” (Figure 1) to tens of femtoseconds that molecules take to vibrate. Ultrafast imaging, therefore, is essential for the observation and characterization of such dynamic events. The ever-increasing demand for a high-temporal resolution in molecular biology is ascribed to the fact that even a slow-motion appears to be “fast” at microscopic scales. For example, to observe an object that travels at a constant speed across a characteristic length, the camera needs a temporal resolution of. Therefore, the smaller the characteristic scale, the finer the required temporal resolution. To image an object, which moves at a “slow” speed ($= 1 \text{ m/s}$) in the sense of human, across $1 \mu\text{m}$ distance, we need a temporal resolution of $(1 \mu\text{m})/(1 \text{ m/s}) = 1 \mu\text{s}$, which corresponds to a rate of one million frames per second (fps).

Since most transient molecular events are a consequence of a cascade of molecular interactions rather than occurring in

isolation, the lack of images limits the scope of the analysis. On the other hand, despite the capability of capturing two-dimensional (2D) images, ventional cameras based on electronic image sensors, such as the charge-coupled device (CCD) and complementary metal-oxide-semiconductor (CMOS), fall short in providing a high frame rate under desirable imaging conditions. The major obstacle is the data transfer speed from an electronic image sensor to the host computer. Using high-speed interfaces such as camera link or peripheral component interconnect (PCI) express, a high-speed camera with one million pixels can stream digitalized images to a computer at only ~ 100 fps. Moreover, the limited memory storage restricts the temporal sequence depth to a few hundred frames, resulting in a very short observation time window. This electronic bandwidth problem further escalates in three-dimensional (3D) imaging, prohibiting a volumetric frame rate beyond tens of frames per second.

Dr. Liang Gao's group at UCLA is pioneering the development of ultrafast optical imagers for bioimaging applications. Recently, his team has developed an innovative ultrafast imaging method, dubbed Light Field Tomography (LIFT), which can perform first-ever 3D snapshot transient imaging at billions of frames per second with full-fledged light field imaging capabilities, including depth retrieval, post-capture refocusing, and extended depth of field (Feng and Gao, 2021). The LIFT can replace the camera in a digital imaging system, allowing one to add high-speed 3D acquisition capability to various imaging modalities. The motivation to develop the LIFT technique comes from the need for speed in light field imaging. To acquire the depth information, conventional light field cameras measure a



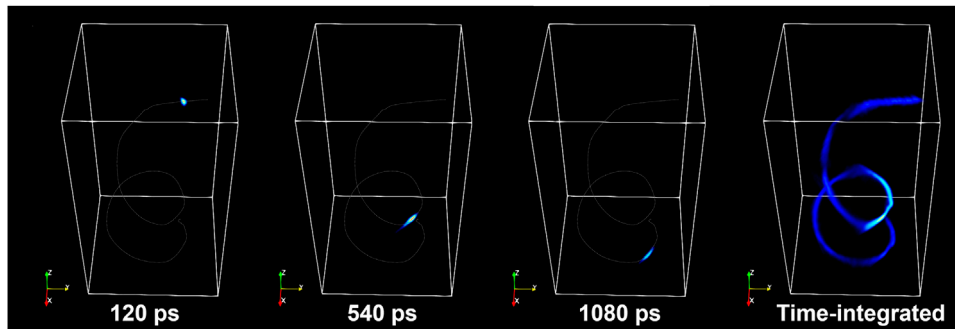


FIGURE 3 | 3D imaging of a laser pulse flying through a spiral fiber-optic cable at light speed. Image courtesy of Liang Gao's lab at UCLA.

complete four-dimensional (4D) plenoptic function (ω), (spatial coordinates, emittance angles), resulting in a large dataset (Gao and Wang, 2016; Zhu et al., 2018). The measurement of such big data requires a large-format image sensor, which usually has a low frame rate. For example, a state-of-the-art light field camera can acquire 3D images at only tens of frames per second⁴. Solving this “big data” problem in light field imaging requires a new light-field sampling scheme in the observation of two facts. First, in most application scenarios, the ultimate goal is to acquire a 3D image, rather than a complete 4D plenoptic function. Second, the perspective images acquired by a conventional light field camera contain almost the same image content: there is only a depth-dependent disparity between any two sub-aperture images. LIFT solves this data redundancy problem by employing nonlocal image acquisitions (i.e., en-face projection) and distributing them into different views. This leads to a measurement dataset much

smaller than a single sub-aperture image, thereby significantly reducing the data load and allowing fast camera readout.

In a typical LIFT camera, the input scene is imaged by an array of cylindrical lenses with various orientations with respect to a linear detector array (Figure 2A). The perspective image acquired by a cylindrical lens is a convolution of a re-scaled geometric image of the object seen from the corresponding view angle and the line spread function of the cylindrical lens (Figure 2B). The cylindrical lenses, therefore, spatially extend the signals emitted from each object point to the linear detector array so they can be simultaneously measured. The resultant 1D image is essentially an *en-face* projection of the object at the orientation angle of that cylindrical lens.

As a niche application, Dr. Gao's group demonstrated LIFT in snapshot transient imaging of light on the fly in 3D (Figure 3) and real-time none-line-of-sight (NLOS) imaging of fast-moving

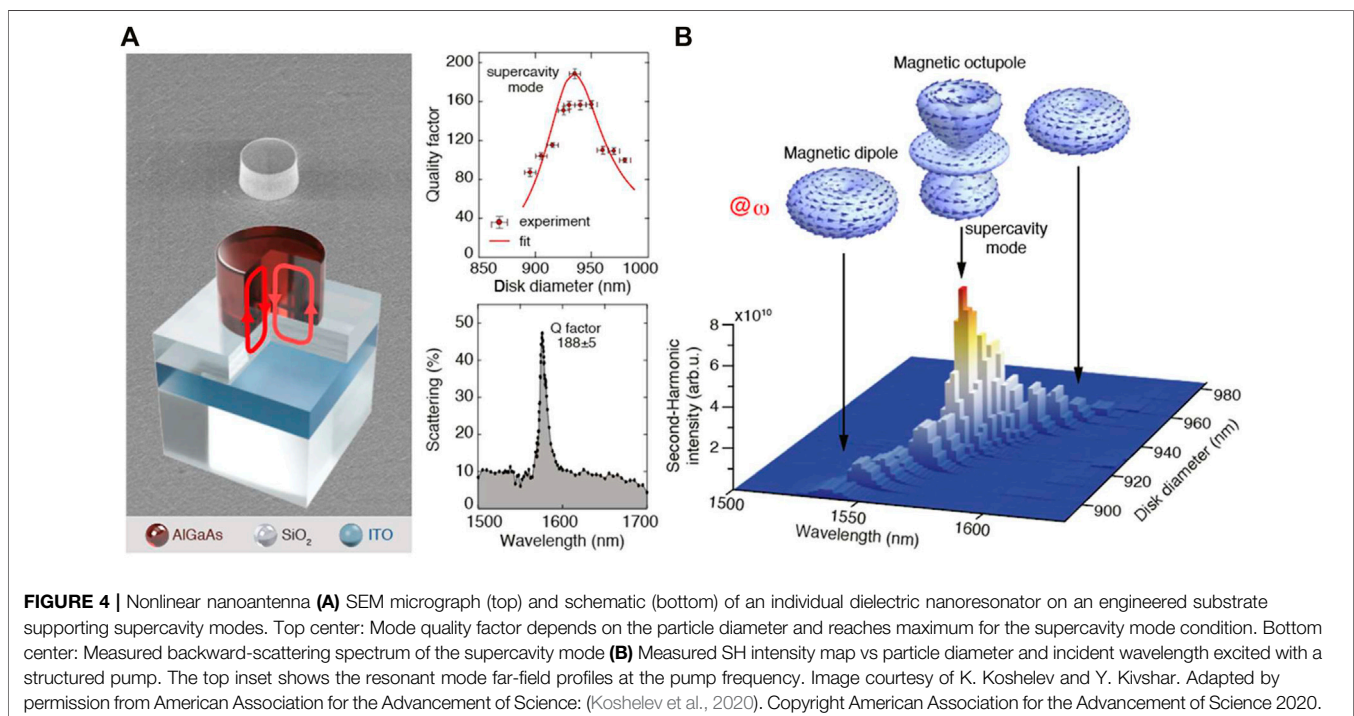


FIGURE 4 | Nonlinear nanoantenna (A) SEM micrograph (top) and schematic (bottom) of an individual dielectric nanoresonator on an engineered substrate supporting supercavity modes. Top center: Mode quality factor depends on the particle diameter and reaches maximum for the supercavity mode condition. Bottom center: Measured backward-scattering spectrum of the supercavity mode (B) Measured SH intensity map vs particle diameter and incident wavelength excited with a structured pump. The top inset shows the resonant mode far-field profiles at the pump frequency. Image courtesy of K. Koshelev and Y. Kivshar. Adapted by permission from American Association for the Advancement of Science: (Koshelev et al., 2020). Copyright American Association for the Advancement of Science 2020.

hidden objects, which are previously impossible without the LIFT technique.

Dr. Gao's team is currently adapting the LIFT technology for microscopic imaging of biological events with a particular interest in 3D fluorescence lifetime imaging microscopy (FLIM). FLIM relies on fluorescent molecules that temporarily light up and glow for only a few billionths of a second (**Figure 1**). This extremely short time frame varies for different molecules, so it can be used as a fingerprint of sorts to detect which target molecules are present and their precise location in biological cells or tissues. Due to a lack of appropriate ultrafast 3D imaging tools, so far, FLIM has been primarily used in imaging 2D biological samples. The application LIFT in FLIM will break this convention, ushering the field into a new 3D era. Despite still being in the early development stage, we expect this one-of-a-kind ultrafast imaging method will bring an astonishing advance to biophotonics, inaugurating a critical pathway to analyze dynamic biological events occurring at a super-fast time scale, including those we have not foreseen yet.

SPOT LIGHT IN NONLINEAR OPTICS

Subwavelength dielectric resonators for nonlinear nanophotonics, by K. Koshelev, S. Kruk, E. Melik-Gaykazyan, J-H Choi, A. Bogdanov, H-G and Y. Kivshar (Koshelev et al., 2020).

The recent developments of nanoscale resonators with strong light confinement opened a pathway towards efficient nonlinear processes on subwavelength scales (Kruk and Kivshar, 2017). In the past, nonlinear nanophotonics was attributed solely to metallic nanoparticles. However, the efficiency of nonlinear frequency conversion in metal nanostructures remains small, being of the order of $\sim 10^{-11}$. All-dielectric resonant nanostructures have recently been suggested as a novel concept to boost nonlinear effects at the nanoscale beyond the limits associated with plasmonics (Koshelev and Kivshar, 2021). Yet, the enhancement of near-field effects for individual subwavelength resonators is strongly limited by the low quality factor (Q factor) of the fundamental resonances governing the optical response.

Recently, a novel theoretical approach (Rybin et al., 2017) was suggested to achieve high-Q resonances in individual dielectric nanoresonators in the regime of supercavity modes by employing the physics of genuine non-radiative states—optical bound states in the continuum (BICs - **Figure 4**). Later, supercavity modes were shown theoretically to provide a giant second-harmonic generation (SHG) due to a strong resonant field enhancement (Carletti et al., 2018).

Very recently, Kruk et al. reported on the experimental observation of the record-high efficiency of SHG from isolated AlGaAs nanodisk resonators in the regime of supercavity mode excitation (Koshelev et al., 2020). First, they observed a supercavity mode at 1585 nm in linear reflection measurements. They designed and fabricated AlGaAs cylindrical resonators with height 635 nm placed on a silica substrate with an additional highly doped 300 nm ITO layer, shown in Figure on the left panel. The ITO layer provides an additional enhancement of the Q factor due to the interaction

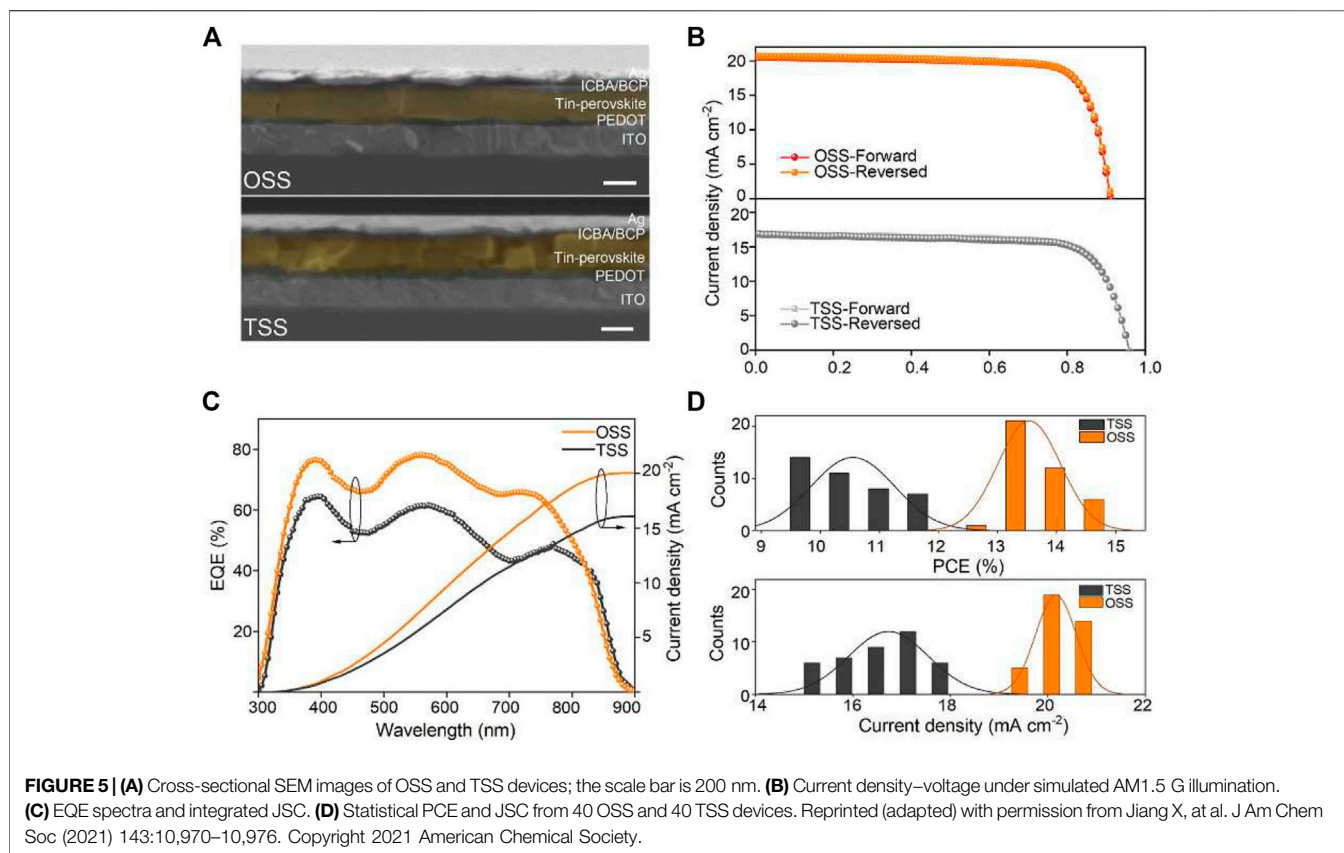
between the resonator and the substrate. To engineer the supercavity mode, they fabricated a set of resonators with the diameter ranging between 890 and 980 nm to induce strong coupling between a pair of Mie modes. For an efficient excitation, they use a tightly focused azimuthally polarized vector beam with the wavelength varying from 1,500 nm to 1,700 nm. As shown in the central panel of Figure, the highest measured Q factor of about 190 was found for the particle with diameter 935 nm, which is more than one order of magnitude higher than for conventional dipolar Mie modes.

SHG nonlinear measurements were performed for the optimized sample. On the right panel of Figure, the map of the SHG intensity versus the pump wavelength and resonator diameter is shown for the nanoresonators pumped by the azimuthal-polarized beam. The experimental data reveal a sharp enhancement of the nonlinear signal in the vicinity of the supercavity mode wavelength. The SH signal is normalized over a spectral function of the setup, which includes filter transmittance, laser power, and detector sensitivity spectra. The origin of the SH signal is verified by the direct measurement of its spectrum (by a visible spectrometer Ocean Optics QE Pro) and its power dependence which is in a quadratic manner. The directly measured conversion efficiency is $1.3 \times 10^{-6} \text{ W}^{-1}$ which is the record-high value of the harmonic generation compared to all previous demonstrations with isolated subwavelength resonators. Individual high-Q dielectric nanoresonators supporting supercavity modes promise specific applications as nonlinear nanoantennas, low-threshold nanolasers, and compact quantum sources.

SPOT LIGHT IN PHOTOVOLTAIC MATERIALS

One-Step Synthesis of $\text{SnI}_2\cdot(\text{DMSO})_x$ Adducts for High-Performance Tin Perovskite Solar Cells, by X. Jiang, H. Li, Q. Zhou, Q. Wei, M. Wei, L. Jiang, Z. Zhang, Z. Peng, F. Wang, Z. Zhang, K. Xu, Y. Hou, S. Teale, W. Zhou, R. Si, X. Gao, E. H. Sargent, Z. Ning (Jiang et al., 2021).

The past 10 years have seen the rapid emergence of organic-inorganic lead halide perovskite solar cells, with their power conversion efficiency (PCE) increasing from 3.8% in 2009 to 25.5% in 2020, comparable to the record efficiencies of c-Si (Kim et al., 2019; Green et al., 2021). Detailed techno-economic analysis has also demonstrated that perovskite photovoltaic technology is potentially very cost-effective because of their low-temperature solution processibility and small materials consumption (Chang et al., 2018). However, the reliance on lead (Pb), as a key perovskite component, may hinder the deployment of Pb-based perovskite technology in consumer or building-integrated applications, as well as in the areas where the use of lead in devices is restricted. Therefore, the substitution of Pb with less toxic elements has been an important research topic in thin-film photovoltaics community and promptly followed the development of Pb-based perovskite solar cells (Chen et al., 2012; Hao et al., 2014). Tin (Sn) is the most promising element that can replace Pb in



the halide perovskite structure due to their proper Goldschmidt's tolerance factor (ranging from 0.85–0.95), excellent optical and electrical properties. Despite the intensive research effort on the development of Sn-based perovskite solar cells, the device performance still lags far behind their Pb-based counterparts due to the major challenges associated with the materials, e.g. oxidation of Sn²⁺ to Sn⁴⁺ increasing recombination centres and fast crystallization process resulting in poor film morphology and quality. Recently, Xiangyuan Jiang, Zhijun Ning and their coworkers have generationally improved Sn-perovskite cell performance through a highly coordinated SnI₂·(DMSO)_x adduct formation in the perovskite precursor (Jiang et al., 2021). They found that by incorporating I₂ in dimethyl sulfoxide (DMSO), I and O in DMSO form a weak bond that facilitates the formation of a SnI₂·(DMSO)_x adduct. The researchers developed a one-step spin-coating (OSS) process by incorporating this SnI₂·(DMSO)_x adduct in the perovskite precursor and demonstrated highly regulated crystal growth enabled by the adduct, which eliminates the formation of SnI₂, a well-known impurity, and pinholes in the film as shown in **Figure 5**. This leads to a longer diffusion length of 290 ± 20 nm compared to 210 ± 20 nm for the conventional two-step spin-coated (TSS) film. Their devices fabricated via the one-step process have achieved a certified efficiency of 14.6%, a ~20% increase compared to the previously reported certified best-performing Sn-halide perovskite solar cells. Even though the device efficiency is still lagging behind the state-of-

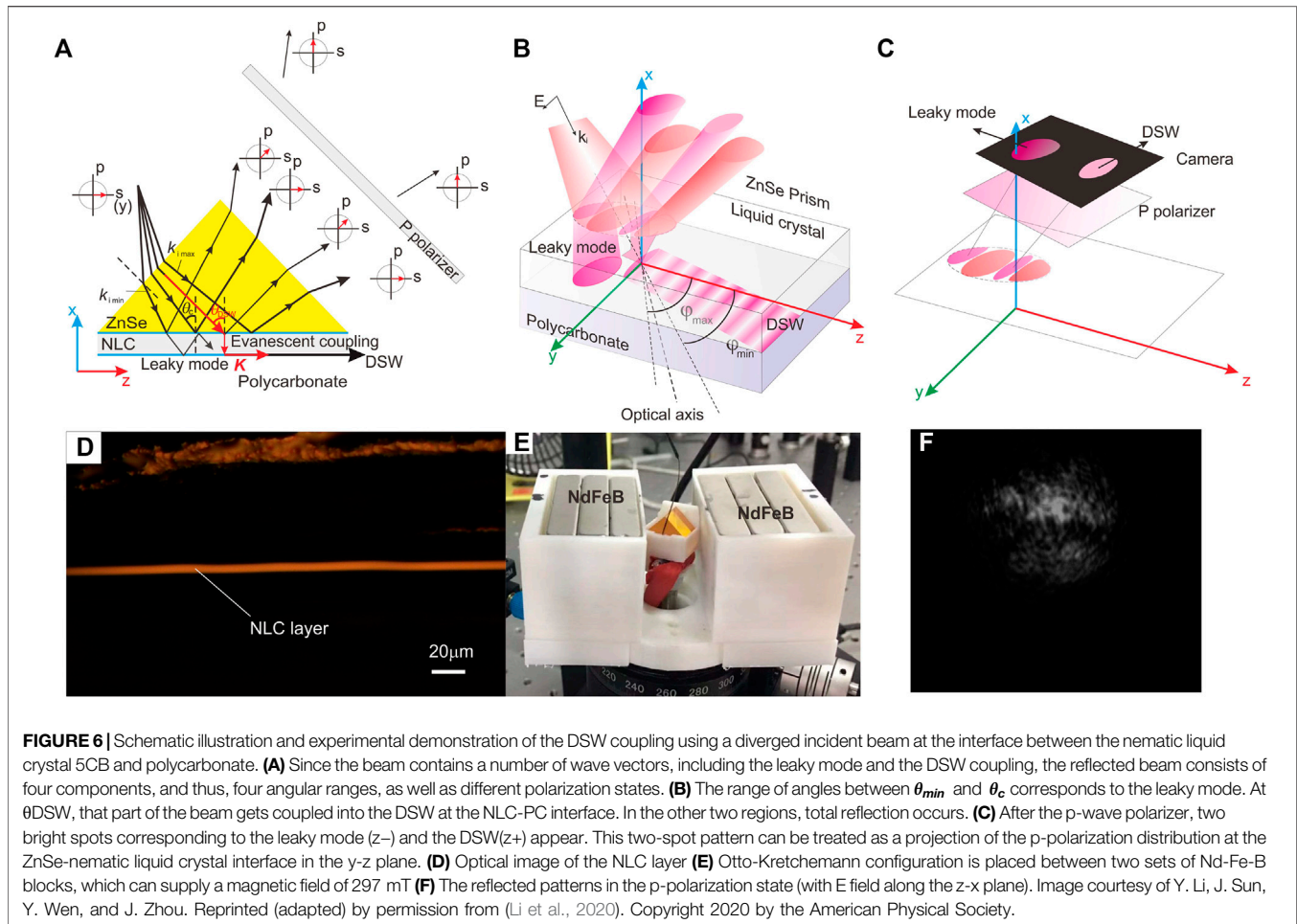
the-art Pb-based perovskite cells, this work has demonstrated a significant progress in Pb-free perovskite devices, directing and motivating further improvement in the future.

SPOT LIGHT IN OPTICAL NANOSTRUCTURES

Controllable Selective Coupling of Dyakonov Surface Waves at a Liquid-Crystal-Based Interface by Y. Li, J. Sun, Y. Wen, and J. Zhou (Li et al., 2020).

Dyakonov surface waves (DSWs) are a type of electromagnetic waves that travel along the interface of an isotropic optical medium n_c and an anisotropic one with a uniaxial refractive index tensor (n_o, n_o, n_e) with an optical axis parallel to the interface, where n_o and n_e are the refractive indices for the ordinary and extraordinary waves, respectively (D'yakonov, 1988). Dyakonov surface waves exist only in a narrow range of dielectric permittivities when $n_o < n_c < n_e$ with the direction of propagation of the DSWs defined by these refractive indices. It is also noteworthy that the DSWs propagate at the interface as a beam with an extremely narrow range of propagation angles, $\Delta\theta < 1^\circ$. Fulfilling the above requirement on the refractive indices and narrow angular range of existence made experimental observation of the DSWs rather challenging.

Indeed, predicted over 30 years ago by Russian physicist Mikhail Dyakonov, the DSWs have been demonstrated for the



first time only in 2009 the interface between potassium titanyl phosphate crystal with biaxial permittivity and an isotropic liquid medium with high refractive index (Takayama et al., 2009).

One of the remarkable advantages of the DSWs over the well-known surface plasmon polaritons (SPP) is that the DSWs propagate at the interface of two transparent media, and therefore, are lossless. In contrast, SPPs propagate at the surface of a metal, i.e. the electric field of SPPs partially resides in the metal, and as a result, experience significant propagation losses and strong dispersion.

To date, several naturally existing and nano-engineered optical materials combinations have been shown to support the DSWs (Takayama et al., 2014; Matsui, 2015; Takayama et al., 2017; Moradi and Niknam, 2018; Li et al., 2020). However, manipulating and steering the DSWs on demand is still challenging. In a recent experimental study, Li et al. (2020) demonstrated a possibility of strongly selective and precise control of input coupling of the DSWs at the interface between the nematic liquid crystal 5CB and polycarbonate (**Figure 6**). The authors showed that those same properties that make the DSWs difficult to observe, simultaneously make them excellent candidates for enabling precisely controlled beam steering and manipulation functionalities!

Nematic liquid crystals offer a unique combination of very strong anisotropy and a magnetically controlled steering of the DSWs. In the presence of an applied magnetic field, the liquid crystal exhibited a uniaxial positive birefringence $n_e = 1.6889$ and $n_o = 1.5438$, with its axis aligned along the magnetic field (Abbate et al., 2007). As the optical axis of the nematic liquid crystal rotated with an applied magnetic field, different angular components of the divergent incident beam were selectively coupled into the surface wave. Demonstrated selective coupling combined with the highly-directional, lossless propagation of the DSWs is likely to open new avenues for manipulating surface-waves, potentially enabling reconfigurable or switchable devices for photonic integrated circuits.

SPOT LIGHT IN OPTICAL INFORMATION PROCESSING AND HOLOGRAPHY

Lenslet VR: Thin, Flat and Wide-FOV Virtual Reality Display Using Fresnel Lens and Lenslet Array by K. Bang, Y. Jo, M. Chae and B. Lee (Bang et al., 2021).

The technology of virtual reality (VR) allows users to see both a real physical world and a virtual world at the same time. Objects

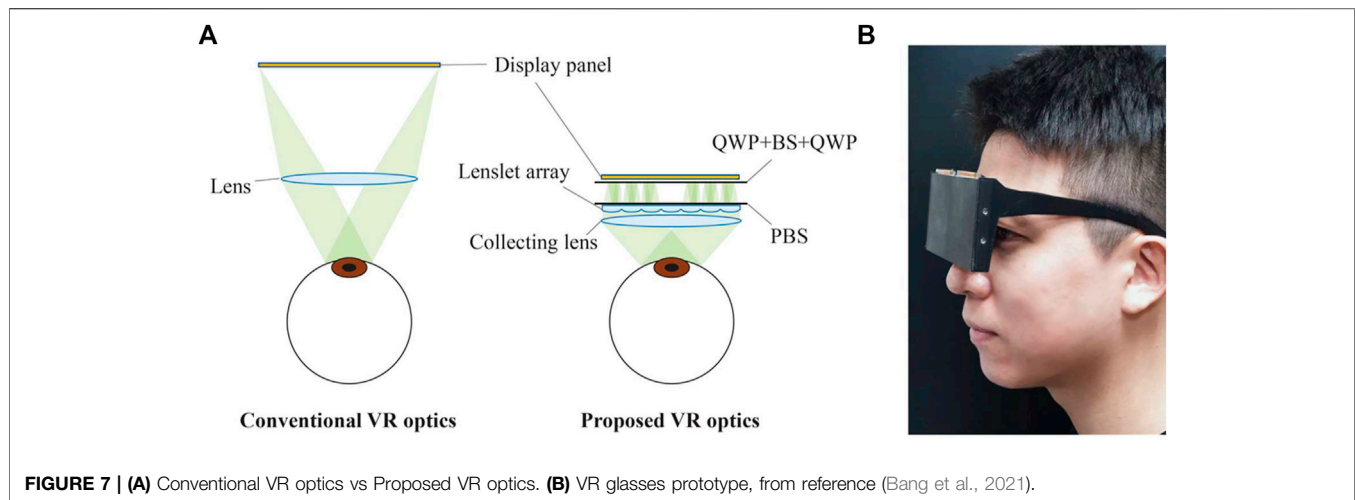


FIGURE 7 | (A) Conventional VR optics vs Proposed VR optics. **(B)** VR glasses prototype, from reference (Bang et al., 2021).

in the virtual world do not exist in the real world. The concept of virtual reality (VR) has been around for a long time and continued to draw much attention because of its huge potential applications in entertainment (such as gaming in games and sports), education (such as medical or military training) and business (such as virtual meetings). However, VR has not yet reached the mainstream. Among other factors such as high cost, insufficient content, limited display quality, one of the main bottlenecks is due to its heavy and bulky headset-type hardware with limited field of view (FOV).

The paper of Bang et al. has designed a thin and wide field-of-view VR near-eye display by using a Fresnel lens and a lenslet array. The focal length of the optics determines display performance. Unlike bulk optics using a single lens to perform imaging as well as collection of the light from the panel to the eye-box (see the left panel of **Figure 7**, from (Bang et al., 2021)), the lenslet array provides short focal length due to the small aperture of each lenslet and the Fresnel lens is used for the collection of the light to the eye box. Roughly speaking, the eye box is the volume of space within which a viewable image is formed by a lens system. The combination of the lenslet and the Fresnel lens provide design flexibility as well as a shorter focal length in the system, i.e., a design which combines two “lenses” instead of a single lens of a fixed focal length. Having a short focal length is important as it will provide wide FOV as, where is the linear dimension of the eye box and is the focal length of the system. In addition, the authors have realized the polarization-based optical folding technique to reduce the required space for imaging (see the right panel of **Figure 7A**). This is done by utilizing a beamsplitter (BS) sandwiched by two quarter wave plates (QWPs) and a polarizing beam splitter (PBS). By reflecting a linearly polarized light from a single pixel of the LCD panel from the PBS and then reflecting once from the BS toward the lenslet array, they have obtained an effective optical path three times longer than the physical distance between the display panel and the lenslet array, effectively reducing the physical required system distance to 1/3 of the required optical system distance. The end result of these designs demonstrates a thin, flat and wide-FOV VR display. Only 3.3 mm of physical distance is required between the

display panel and the lens. The integrated VR display can have a compact form factor like sunglasses as shown in **Figure 7B**. While the thin and flat VR design has been met, certain issues exist, such as aberration from the Fresnel lens and blurry background noise due to the undesired reflection and transmission of the optical folding technique.

Palm-sized single-shot phase-shifting incoherent digital holography system by T. Tahara and R. Oi (Tahara and Oi, 2021).

The term “holographic fluorescence microscopy” was coined in 1997 when holograms of fluorescent specimens were recorded for the first time (Schilling et al., 1997). Indeed that was the milestone of digital incoherent holography, and the capability of being able to capture fluorescence information is of particular importance for biomedical applications as over 90% of specimens are fluorescent. In incoherent holography, we capture the intensity distribution of a 3-D object holographically. Holographic fluorescence microscopy is accomplished by the principle optical scanning holography (OSH) (Poon, 1985). A non-scanning motionless fluorescence holographic microscope was demonstrated in 2008 (Rosen and Brooker, 2008). The technique is based on Fresnel incoherent correlation holography (FINCH), and the principle of FINCH is based on the concept of what we now call self-interference (Poon, 2008). Nowadays, OSH and FINCH are two major and well-known incoherent digital holographic techniques. The digital incoherent holographic system reported by the author represents a state-of-the-art FINCH system in terms of physical size. A palm-sized system having dimensions of 30 mm × 35 mm × 50 mm (including the camera) is shown in **Figure 8A**) and its schematic is shown in **Figure 8B**). Being a palm-sized system is essential for portable 3D microscopy applications. The polarization system employs two thin geometric phase lenses to achieve interference of two spherical waves of different curvatures to perform self-interference. The system also incorporates a micro-polarizer array to achieve single-shot recording instead of conventional FINCH recording where at least three holograms are needed to achieve a complex hologram recording. **Figure 9A**) shows a reflective object with 7-mm width and 193 mm away from the system, and **Figure 9B**) shows a

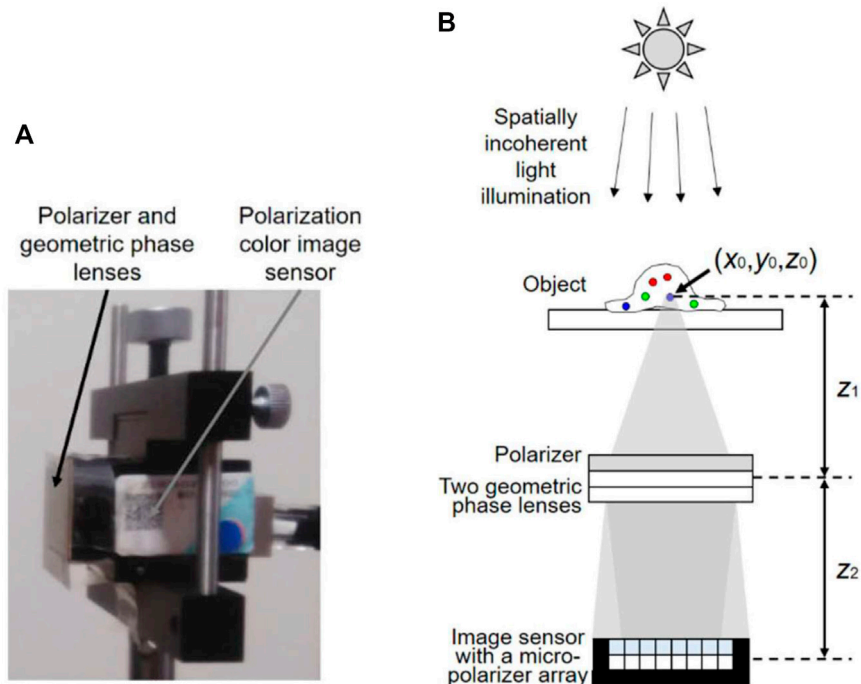


FIGURE 8 | (A) Photograph of the incoherent digital holography system (IDHS) of size 30 mm x 35 mm x 50 mm. **(B)** Schematic of the IDHS. Reprinted (adapted) with permission from ref (Schilling et al., 1997) © Optica Publishing Group.

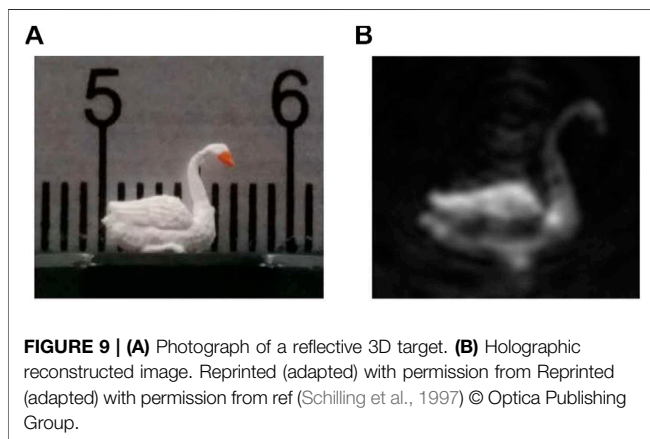


FIGURE 9 | (A) Photograph of a reflective 3D target. **(B)** Holographic reconstructed image. Reprinted (adapted) with permission from Reprinted (adapted) with permission from ref (Schilling et al., 1997) © Optica Publishing Group.

focused reconstructed image. The constructed microscopic system has a resolution of about 10 μm . Field of view and resolution improvements are the next goals.

SPOT LIGHT IN TERAHERTZ AND MICROWAVE PHOTONICS

High power portable THz laser systems by Ali Khalatpour, Andrew K Paulsen, Chris Deimert, Zbig R Wasilewski, Qing Hu (Khalatpour et al., 2021).

For the past 4 decades the Terahertz (THz) region of the electromagnetic spectrum has been defined as the “THz gap” due

to the lack of compact, powerful coherent sources. Recently, a significant progress has been made towards the goal of an on-chip, portable laser source that will finally unlock the different potential applications. First, the demonstration of thermoelectric-cooled quantum cascade lasers in 2019 (Bosco et al., 2019; Kainz et al., 2019) and, 1 year later, the breakthrough from the MIT group led by Qing Hu of a THz quantum cascade laser operating up to 250 K on a single-stage thermoelectric cooler (Khalatpour et al., 2021). These major advancements have been possible thanks to a highly focused effort in the understanding and the optimization of all the aspects involving the device design and fabrication. The quantum cascade laser (Faist et al., 1994; Köhler et al., 2002) is a semiconductor laser based on intersubband transitions in the conduction band of a III-V semiconductor. The optical gain and the emission frequency can be tailored by quantum engineering and do not depend on the bandgap of the semiconductor materials constituting the heterostructure. In the case of the THz devices, the GaAs/AlGaAs material system proved to be the most successful for the production of high temperature operating devices. The main difficulties to overcome are the selective injection of electrons in the upper state of the lasing transition since the energy spacing (10–20 meV) is comparable to the broadening at 300 K, and the selective depopulation of the lower state. In the last decade the efforts have been concentrated on a very simple design architecture comprising only two quantum wells (Scalari et al., 2010), in stark contrast with the early developments where many quantum wells were employed (Köhler et al., 2002).

In their paper, Khalatpour et al. Present an improved version of the two-quantum well design based on an GaAs/Al_{0.3}Ga_{0.7}As heterostructure. The band structure of such a device is reported in

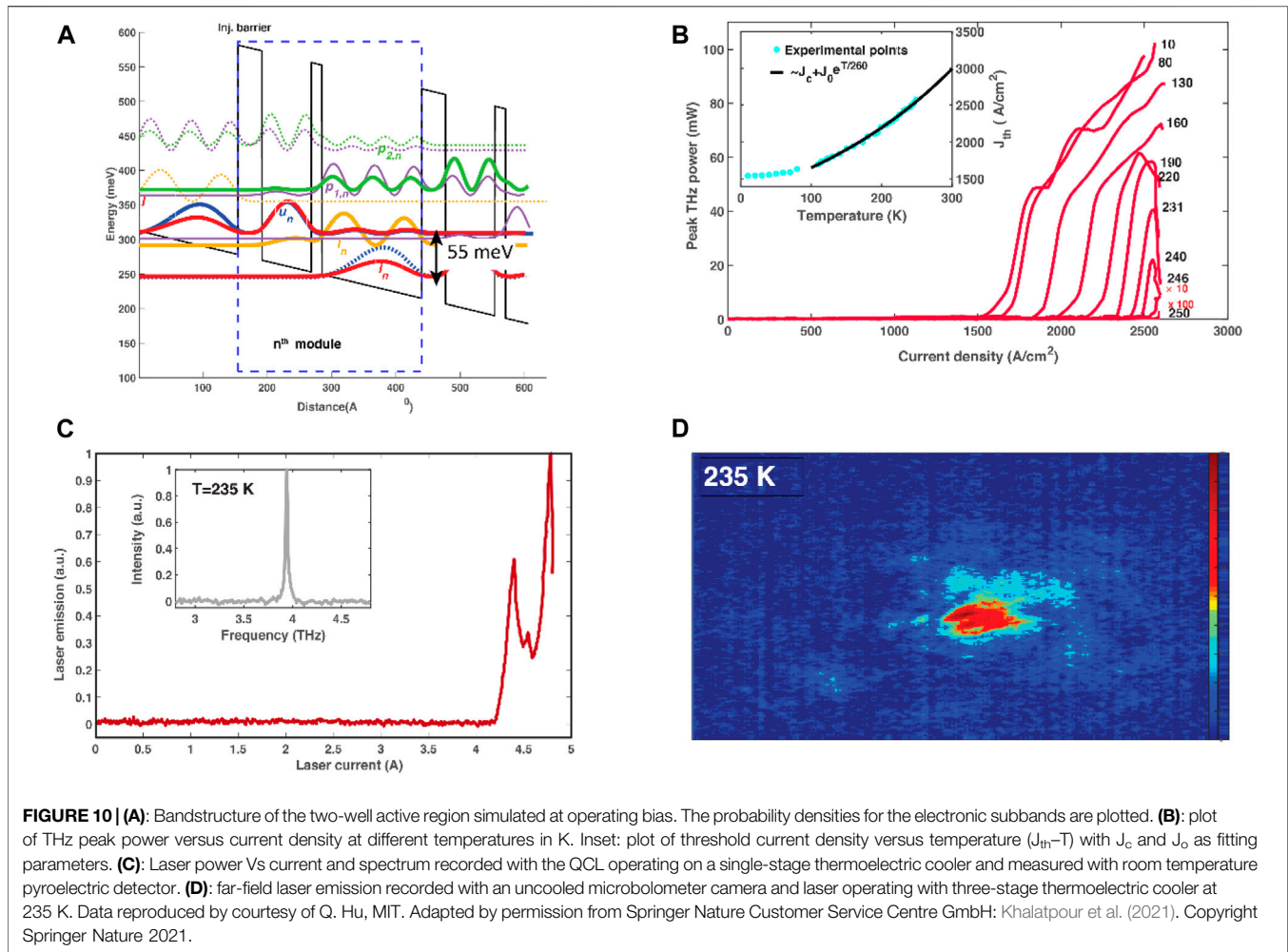


Figure 10A, where the upper lasing state is marked with u_n and the lower with l_n . The lasing frequency is four THz, corresponding to an energy of about 16.5 meV. The key steps that allowed the high temperature operation of are the increased band offset provided by the 30% Aluminum alloy barriers that limits the leakage currents of electrons in the continuum and a deep well for electron extraction from the lower state with an energy spacing of 55 meV, much larger than the optical phonon energy (36 meV) that was used in previous structures.

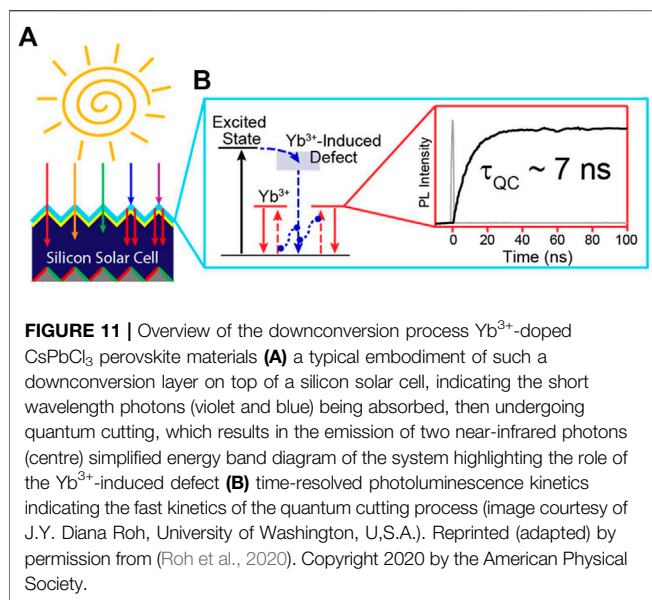
The robust temperature behavior of the laser is highlighted by the very high value of the $T_0 = 260$ K that fits the current density dependence from the temperature (**Figure 10B**). Even though operated at low duty cycles (<1%) the laser displays an impressive peak power in excess of 20 mW at 240 K. Such high power values allow the recording of spectra with room temperature detectors (**Figure 1C**) with the device cooled by a single-stage thermoelectric element. Especially important for applications in the field of imaging is the possibility to use video-rate uncooled cameras in combination with the THz QCL to produce THz images with both laser and camera operating above 230 K. It has to be underlined that these QC THz lasers are semiconductor injection lasers with typical device dimensions of 1–3 mm length and some 100–200 μm width.

The advancement brought by the work of Qing Hu's group at MIT constitutes then a major step towards the integration of these powerful THz sources in portable devices that can be deployed in the field and eventually constitute the source for future, short range, ultrawide bandwidth telecommunication systems (6G and beyond).

SPOT LIGHT IN LIGHT SOURCES AND LUMINESCENT MATERIALS

Yb³⁺ speciation and energy-transfer dynamics in quantum-cutting Yb³⁺-doped CsPbCl₃ perovskite nanocrystals and single crystals by J.Y.D. Roh, M.D. Smith, M.J. Crane, D. Biner, T.J. Milstein, K.W. Krämer and D.R. Gamelin (Roh et al., 2020).

Spectral conversion materials offer the possibility of enhancing the performance of solar energy harvesting systems. In particular, up-conversion and down-conversion afford the possibility of being able to overcome intrinsic loss mechanisms in solar cells, which result in the so-called Shockley-Queisser efficiency limit (Shockley and Queisser, 1961). The addition of an up-conversion layer to the rear of semi-transparent single-junction solar cells allows for sub-bandgap photons to be



harvested, although the nonlinear nature of the mechanism makes this challenging under terrestrial sunlight (Richards et al., 2021). However, the converse approach of down-conversion—whereby each high energy photon is “cut” into two lower energy photons—has long captured the imagination of researchers (Trupke et al., 2002; Richards, 2006) seeking to overcome thermalization losses within solar cells. The left-hand schematic in **Figure 11** illustrates that such a down conversion layer could be placed on top of a silicon solar cell, enabling each high energy photon (above a certain energy threshold) to be split into two lower-energy photons, thereby enhancing both the external quantum efficiency of the device at short wavelengths and also, overall, the generated photocurrent density. For those readers more familiar with organic or quantum dot materials, the down-conversion process described here is similar to singlet fission or multiple exciton generation. However, these approaches face considerable challenges with the excitation of the energy challenges due to competition via non-radiative recombination channels.

In the last 5 years, the group of Prof. Daniel Gamelin at the University of Washington, U.S.A., has made exciting progress in realizing down-conversion systems exhibiting an internal photoluminescent quantum yield (PLQY) of well over 190% (Kroupa et al., 2018). A slight dampener on the immediate applicability of such performance-enhancing layers to photovoltaics was encountered when the group determined that under the photon flux that is typical for terrestrial sunlight, the PLQY drops to closer to 100% (Erickson et al., 2019).

In the spot-lighted paper (Roh et al., 2020), J.Y. Diana Roh and others investigate the fundamental origins of down-conversion—also known as quantum cutting—in depth. In particular, the studies presented indicate very little differences between the ytterbium-doped metal halide perovskite ($\text{CsPbCl}_3:\text{Yb}^{3+}$) material, whether it is a nanocrystal or a single crystal. The photophysical studies demonstrate that efficient down-conversion is, indeed, an intrinsic property of the material. This is good news for the

engineering of such layers and applying them to silicon solar cells, as either a polymeric layer containing nanocrystals or continuous thin film would be possible.

Furthermore, Roh *et al.* conducted time-resolved photoluminescence spectroscopy measurements, with the results indicating that an intermediate state—that was previously hypothesized to exist—indeed does play an important role in the downconversion mechanism. This intermediate state is attributed to a Yb^{3+} induced defect and assists in the energy transfer from the photogenerated excited state of the perovskite down to the excited state of Yb^{3+} that is responsible for emission (**Figure 11**). Upon excitation of the perovskite with, for example, violet light (404 nm), quantum cutting can proceed efficiently via two consecutive energy-transfer steps. Firstly, energy is transferred from the exciton to a shallow dopant-induced defect. This depopulation process is very fast (single-picosecond timescale), thus allowing it to effectively compete with other non-radiative recombination processes. Secondly, energy is transferred from the latter defect state to a pair of Yb^{3+} ions. This step is also very fast, having a lifetime of ~ 7 ns at room temperature.

The key challenge that remains is the long-lived (>1 ms) lifetime of the Yb^{3+} excited state, which causes a bottleneck that ultimately results in saturation of the PLQY at the high photon fluxes, e.g. those encountered under terrestrial sunlight. While Roh *et al.* have observed that elevated temperatures result in a slight reduction in this lifetime—and that such temperatures (up to 80°C) are encountered for silicon solar cells operating in desert-like environments—however, the main challenge is that the increased photocurrent realized via down-conversion will be counteracted by a drop in photovoltage (typically -2.2 mV/ $^\circ\text{C}$ for a silicon device).

Thus, before the holy grail of down-conversion layers boosting the performance of silicon photovoltaics can be realized, the bottleneck of the long lifetime of the Yb^{3+} emitting state needs to be overcome. Yet, exciting progress is being made!

AUTHOR CONTRIBUTIONS

All the authors contributed to the general setting of the review and the identification of the spot-lighted papers. In particular BA, CA, SH, NL, T-CP, GS and BR led the drafting of the Spot Light in Biophotonics, Spot Light in Nonlinear Optics, Spot Light in Photovoltaic Materials, Spot Light in Optical Nanostructures, Spot Light in Optical Information Processing and Holography, Spot Light in Terahertz and Microwave Photonics, Spot Light in Light Sources and Luminescent Materials, respectively. MP supervised the overall organization, drafting and finalization of the paper.

ACKNOWLEDGMENTS

The authors are indebted to all the authors of the spot-lighted papers for providing feedback on their outputs and to the American Chemical Society, American Physical Society, the American Association for the Advancement of Science, the Optica Publishing Group and Springer Nature for providing the necessary reprint permission, where required.

REFERENCES

- Abbate, G., Tkachenko, V., Marino, A., Vita, F., Giocondo, M., Mazzulla, A., et al. (2007). Optical Characterization of Liquid Crystals by Combined Ellipsometry and Half-Leaky-Guided-Mode Spectroscopy in the Visible-Near Infrared Range. *J. Appl. Phys.* 101, 073105. doi:10.1063/1.2714768
- Bang, K., Jo, Y., Chae, M., Lee, B., and Lenslet, V. R. (2021). Lenslet VR: Thin, Flat and Wide-FOV Virtual Reality Display Using Fresnel Lens and Lenslet Array. *IEEE Trans. Vis. Comput. Graphics* 27, 2545–2554. doi:10.1109/TVCG.2021.3067758
- Bosco, L., Francké, M., Scalari, G., Beck, M., Wacker, A., and Faist, J. (2019). Thermoelectrically Cooled THz Quantum Cascade Laser Operating up to 210 K. *Appl. Phys. Lett.* 115, 010601. doi:10.1063/1.5110305
- Carletti, L., Koshelev, K., De Angelis, C., and Kivshar, Y. (2018). Giant Nonlinear Response at the Nanoscale Driven by Bound States in the Continuum. *Phys. Rev. Lett.* 121, 033903. doi:10.1103/PhysRevLett.121.033903
- Chang, N. L., Ho-Baillie, A. W. Y., Vak, D., Gao, M., Green, M. A., and Egan, R. J. (2018). Manufacturing Cost and Market Potential Analysis of Demonstrated Roll-To-Roll Perovskite Photovoltaic Cell Processes. *Solar Energ. Mater. Solar Cell.* 174, 314–324. doi:10.1016/j.solmat.2017.08.038
- Chen, Z., Wang, J. J., Ren, Y., Yu, C., and Shum, K. (2012). Schottky Solar Cells Based on CsSnI₃ Thin-Films. *Appl. Phys. Lett.* 101, 093901. doi:10.1063/1.4748888
- D'yakonov, M. I. (1988). New Type of Electromagnetic Wave Propagating at an Interface. *J. Exp. Theor. Phys.* 64, 714–716.
- Erickson, C. S., Crane, M. J., Milstein, T. J., and Gamelin, D. R. (2019). Photoluminescence Saturation in Quantum-Cutting Yb³⁺-Doped CsPb(Cl_{1-x}Br_x)₃ Perovskite Nanocrystals: Implications for Solar Downconversion. *J. Phys. Chem. C* 123, 12474–12484. doi:10.1021/acs.jpcc.9b01296
- Faist, J., Capasso, F., Sivco, D. L., Sirtori, C., Hutchinson, A. L., and Cho, A. Y. (1994). Quantum Cascade Laser. *Science* 264 553–556. doi:10.1126/science.264.5158.553
- Feng, X., and Gao, L. (2021). Ultrafast Light Field Tomography for Snapshot Transient and Non-Line-of-Sight Imaging. *Nat. Commun.* 12, 2179. doi:10.1038/s41467-021-22461-0
- Gao, L., and Wang, L. V. (2016). A Review of Snapshot Multidimensional Optical Imaging: Measuring Photon Tags in Parallel. *Phys. Rep.* 616, 1–37. doi:10.1016/j.physrep.2015.12.004
- Green, M., Dunlop, E., Hohl-Ebinger, J., Yoshita, M., Kopidakis, N., and Hao, X. (2021). Solar Cell Efficiency Tables (Version 57). *Prog. Photovolt Res. Appl.* 29, 3–15. doi:10.1002/pip.3371
- Hao, F., Stoumpos, C. C., Cao, D. H., Chang, R. P. H., and Kanatzidis, M. G. (2014). Lead-free Solid-State Organic-Inorganic Halide Perovskite Solar Cells. *Nat. Photon.* 8, 489–494. doi:10.1038/nphoton.2014.82
- Jiang, X., Li, H., Zhou, Q., Wei, Q., Wei, M., Jiang, L., et al. (2021). One-Step Synthesis of SnI₂(DMSO)_x Adducts for High-Performance Tin Perovskite Solar Cells. *J. Am. Chem. Soc.* 143, 10970–10976. doi:10.1021/jacs.1c03032
- Kainz, M. A., Semtsiv, M. P., Tsianos, G., Kurlov, S., Masselink, W. T., Schönhuber, S., et al. (2019). Thermoelectric-cooled Terahertz Quantum cascade Lasers. *Opt. Express.* 27, 20688. doi:10.1364/OE.27.20688
- Khalatpour, A., Paulsen, A. K., Deimert, C., Wasilewski, Z. R., and Hu, Q. (2021). High-power Portable Terahertz Laser Systems. *Nat. Photon.* 15, 16–20. doi:10.1038/s41566-020-00707-5
- Kim, J., Ho-Baillie, A., and Huang, S. (2019). Review of Novel Passivation Techniques for Efficient and Stable Perovskite Solar Cells. *Sol. RRL.* 3, 1800302. doi:10.1002/solr.201800302
- Köhler, R., Tredicucci, A., Beltram, F., Beere, H. E., Linfield, E. H., Davies, A. G., et al. (2002). Terahertz Semiconductor-Heterostructure Laser. *Nature* 417, 156–159. doi:10.1038/417156a
- Koshelev, K., and Kivshar, Y. (2021). Dielectric Resonant Metaphotonics. *ACS Photon.* 8, 102–112. doi:10.1021/acsphotonics.0c01315
- Koshelev, K., Kruk, S., Melik-Gaykazyan, E., Choi, J.-H., Bogdanov, A., Park, H.-G., et al. (2020). Subwavelength Dielectric Resonators for Nonlinear Nanophotonics. *Science* 367, 288–292. doi:10.1126/science.aaz3985
- Kroupa, D. M., Roh, J. Y., Milstein, T. J., Creutz, S. E., and Gamelin, D. R. (2018). Quantum-Cutting Ytterbium-Doped CsPb(Cl_{1-x}Br_x)₃ Perovskite Thin Films with Photoluminescence Quantum Yields over 190. *ACS Energ. Lett.* 3, 2390–2395. doi:10.1021/acsenerylett.8b01528
- Kruk, S., and Kivshar, Y. (2017). Functional Meta-Optics and Nanophotonics Governed by Mie Resonances. *ACS Photon.* 4, 2638–2649. doi:10.1021/acsphotonics.7b01038
- Li, Y., Sun, J., Wen, Y., and Zhou, J. (2020). Controllable Selective Coupling of Dyakonov Surface Waves at a Liquid-Crystal-Based Interface. *Phys. Rev. Appl.* 13, 024024. doi:10.1103/PhysRevApplied.13.024024
- Matsui, T. (2015). Dyakonov Surface Waves in Nanoparticle-Dispersed Liquid crystal Metamaterials. *Appl. Phys. Express.* 8, 072601. doi:10.7567/APEX.8.072601
- Moradi, M., and Niknam, A. R. (2018). Terahertz Dyakonov Surface Waves in Plasma Metamaterials. *Opt. Lett.* 43, 519. doi:10.1364/OL.43.000519
- Poon, T.-C. (1985). Scanning Holography and Two-Dimensional Image Processing by Acousto-Optic Two-Pupil Synthesis. *J. Opt. Soc. Am. A* 2, 521–527. doi:10.1364/JOSAA.2.000521
- Poon, T.-C. (2008). Scan-free Three-Dimensional Imaging. *Nat. Photon.* 2, 131–132. doi:10.1038/nphoton.2008.09
- Richards, B. S., Hudry, D., Busko, D., Turshatov, A., and Howard, I. A. (2021). Photon Upconversion for Photovoltaics and Photocatalysis: A Critical Review. *Chem. Rev.* 121, 9165–9195. doi:10.1021/acs.chemrev.1c00034
- Richards, B. S. (2006). Luminescent Layers for Enhanced Silicon Solar Cell Performance: Down-Conversion. *Solar Energ. Mater. Solar Cell.* 90, 1189–1207. doi:10.1016/j.solmat.2005.07.001
- Roh, J. Y. D., Smith, M. D., Crane, M. J., Biner, D., Milstein, T. J., Krämer, K. W., et al. (2020). Yb³⁺ Speciation and Energy-Transfer Dynamics in Quantum-Cutting Yb³⁺-doped CsPbCl₃ Perovskite Nanocrystals and Single Crystals. *Phys. Rev. Mater.* 4, 105405. doi:10.1103/PhysRevMaterials.4.105405
- Rosen, J., and Brooker, G. (2008). Non-scanning Motionless Fluorescence Three-Dimensional Holographic Microscopy. *Nat. Photon.* 2, 190–195. doi:10.1038/nphoton.2007.300
- Rybin, M. V., Koshelev, K. L., Sadrieva, Z. F., Samusev, K. B., Bogdanov, A. A., Limonov, M. F., et al. (2017). High-Q Supercavity Modes in Subwavelength Dielectric Resonators. *Phys. Rev. Lett.* 119, 243901. doi:10.1103/PhysRevLett.119.243901
- Scalari, G., Amanti, M. I., Walther, C., Terazzi, R., Beck, M., and Faist, J. (2010). Broadband THz Lasing from a Photon-Phonon Quantum cascade Structure. *Opt. Express.* 18, 8043. doi:10.1364/OE.18.008043
- Schilling, B. W., Poon, T.-C., Indebetouw, G., Storrie, B., Shinoda, K., Suzuki, Y., et al. (1997). Three-dimensional Holographic Fluorescence Microscopy. *Opt. Lett.* 22, 1506–1508. doi:10.1364/OL.22.001506
- Shockley, W., and Queisser, H. J. (1961). Detailed Balance Limit of Efficiency of P-n Junction Solar Cells. *J. Appl. Phys.* 32, 510–519. doi:10.1063/1.1736034
- Tahara, T., and Oi, R. (2021). Palm-sized Single-Shot Phase-Shifting Incoherent Digital Holography System. *OSA Continuum.* 4, 2372. doi:10.1364/OSAC.431930
- Takayama, O., Artigas, D., and Torner, L. (2014). Lossless Directional Guiding of Light in Dielectric Nanosheets Using Dyakonov Surface Waves. *Nat. Nanotech.* 9, 419–424. doi:10.1038/nnano.2014.90
- Takayama, O., Crasovan, L., Artigas, D., and Torner, L. (2009). Observation of Dyakonov Surface Waves. *Phys. Rev. Lett.* 102, 043903. doi:10.1103/PhysRevLett.102.043903
- Takayama, O., Shkondin, E., Bogdanov, A., Aryaee Panah, M. E., Golenitskii, K., Dmitriev, P., et al. (2017). Midinfrared Surface Waves on a High Aspect Ratio Nanotrench Platform. *ACS Photon.* 4, 2899–2907. doi:10.1021/acsphotonics.7b00924
- Trupke, T., Green, M. A., and Würfel, P. (2002). Improving Solar Cell Efficiencies by Up-Conversion of Sub-band-gap Light. *J. Appl. Phys.* 92, 4117–4122. doi:10.1063/1.1505677
- Zhu, S., Lai, A., Eaton, K., Jin, P., and Gao, L. (2018). On the Fundamental Comparison between Unfocused and Focused Light Field Cameras. *Appl. Opt.* 57, A1. doi:10.1364/AO.57.0000A1

Conflict of Interest: The authors declare that the research was conducted in the absence of any commercial or financial relationships that could be construed as a potential conflict of interest.

Publisher's Note: All claims expressed in this article are solely those of the authors and do not necessarily represent those of their affiliated organizations, or those of the publisher, the editors and the reviewers. Any product that may be evaluated in this article, or claim that may be made by its manufacturer, is not guaranteed or endorsed by the publisher.

Copyright © 2022 Anvari, De Angelis, Huang, Litchinitser, Poon, Scalari, Richards and Peccianti. This is an open-access article distributed under the terms of the Creative Commons Attribution License (CC BY). The use, distribution or reproduction in other forums is permitted, provided the original author(s) and the copyright owner(s) are credited and that the original publication in this journal is cited, in accordance with accepted academic practice. No use, distribution or reproduction is permitted which does not comply with these terms.